Carbohydrate Polymers 113 (2014) 394–402

Contents lists available at ScienceDirect

Carbohydrate Polymers

journal homepage: www.elsevier.com/locate/carbpol

Spin coated cellulose nanocrystal/silver nanoparticle films

E. Fortunati [a], S. Mattioli [a], I. Armentano [a,*], J.M. Kenny [a,b]

[a] Materials Engineering Center, UdR INSTM, University of Perugia, Str. Pentima 4, 05100 Terni, Italy
[b] Institute of Polymer Science and Technology, CSIC, Juan de la Cierva 3, 28006 Madrid, Spain

ARTICLE INFO

Article history:
Received 21 May 2014
Received in revised form 7 July 2014
Accepted 8 July 2014
Available online 15 July 2014

Keywords:
Cellulose nanocrystals
Silver nanoparticles
Spin coating
Assembled films

ABSTRACT

In this study, thin films of cellulose nanocrystals (CNC) and silver nanoparticles (Ag) were assembled on different substrates by spin coating. The effect of substrates, deposition parameters, and nanocrystal modification on the topographical and hydrophilic properties of the obtained layers was investigated. Dilute concentrations of pristine cellulose nanocrystals (CNC) and surfactant modified crystals (s-CNC) were used in order to evaluate the effect of modification and concentration on the uniformity of the spin coated cellulose/silver layers. Morphological investigations by field emission scanning electron microscopy and atomic force microscopy were performed in order to prove the uniformity of the obtained films, while the wettability of different surfaces were studied and correlated to the cellulose modification and content. The ability of s-CNC to form a stable dispersion in chloroform permits the formation of a uniform cellulose film on the substrate surfaces generating regular films during the spin coating process. Topographical investigations show, on the other hand, that the CNC/Ag suspension produces a non-uniform distribution. These effects can be mainly attributed to the surfactant action rather than to the chemical and electrical properties of the substrate surface. Finally, contact angle studies, underline the hydrophilic nature of s-CNC/Ag based films highlighting that the wettability properties are strongly influenced by the cellulose nanocrystal nature.

1. Introduction

In spin coating, solid films are prepared from a dissolved or dispersed substance by removing the solvent during high-speed spinning. While frequently used at an industrial scale, for instance in microelectronics and optics (Norman, Ghanbari-Siahkali, & Larsen, 2005), the past decades have expanded the use of spin coating as a technique for preparing reproducible ultrathin films for research purposes in, e.g., polymer science (Budkowski, 1999), catalysis research (Gunter, Niemantsverdriet, Ribeiro, & Somorjai, 1997) and nanotechnology (Xia & Brueck, 2004; Sun & Sirringhaus, 2006). Recently, however, the need for development of new and well ordered morphological structures in nanoscience has pressed the use of spin coating to further achievements: periodic arrays of nanoparticles (Xia & Brueck, 2004), ordered nanorod films (Sun & Sirringhaus, 2006), open films of individual polymer molecules (Qin, Matyjaszewski, Xu, & Sheiko, 2003), nanosized cellulose layer (Kontturi, Thüne, Alexeev, & Niemantsverdriet, 2005), oriented colloidal crystals (Jiang & McFarland, 2004) and ordered nanocomposite films (Jiang & McFarland, 2004; Singh & Mukherjee, 2004), simplifying some common laboratory procedures (Lee, Lee, & Hong, 2003; Yoon et al., 2004). Cellulose is a natural carbohydrate polymer consisting of repeated β-D-glucose monomer units (Mark, 1980) and it is considered to be an almost inexhaustible raw material (Kaplan, 1998). With the increasing demand for environmentally friendly products, over the last two decades, a large amount of research has been focused on natural cellulose fibres (Klemn, Heublein, Fink, & Bohn, 2005). Cellulose nanocrystals (CNC) are typically rigid rod-shaped monocrystalline domains with 1–100 nm in diameter and from tens to hundreds of nanometers in length depending on the cellulose source. CNC can be produced by acid hydrolysis of various natural cellulose fibres such as cotton, lignocellulosic materials or marine animal tunicates (Dong, Revol, & Gray, 1998; Edgar & Gray, 2002). There, CNC are commonly produced by the hydrolysis of microcrystalline cellulose (MCC) using sulphuric acid that removes the amorphous cellulose to form highly crystalline cellulose of colloidal dimensions with much smaller size than MCC (Fortunati et al., 2012a,b). Interactions of cellulose fibre surfaces with wet-end additives and other materials, depend both on the interfacial properties of the cellulose and on the morphology of the surface. So, it is useful to separate these two kinds of interactions, those due to the cellulose nature and surfactants,

* Corresponding author. Tel.: +39 0744 492914; fax: +39 0744 492950.
E-mail address: ilaria.armentano@unipg.it (I. Armentano).

http://dx.doi.org/10.1016/j.carbpol.2014.07.010
0144-8617/

and those depending on the surface roughness and porosity. The nanometer-sized width of the rod-like colloidal nanocellulose particles allows a relatively flat surface to be prepared by casting an aqueous suspension on an appropriate substrate and allowing the water to evaporate (Revol, Bradford, Giasson, Marchessault, & Gray, 1992). Cellulose nanocrystals possess unique properties as high mechanical response, biodegradability and biocompatibility, high stiffness and low density. However, cellulose crystals are very difficult to disperse in organic solvents due to their strong hydrogen bonding affecting some possible applications (Turbak, Snyder, & Sandberg, 1983). In a non-polar organic solvent, the electrostatic repulsion is inefficient and the establishment of strong hydrogen bonds between cellulose crystals leads to a rapid aggregation of the colloidal suspension. Some attempts have been made to disperse cellulose crystals in organic solvents by chemical modification of the microcrystal surface. This method is still limited to the dispersion in acetone or acetic acid and requires controlled experimental procedures (Cavailleí, Chanzy, Fleury, & Sassi, 1997). In a different field, the dispersion of boehmite rods in cyclohexane has been reported by chemical grafting of poly(isobutene) (Buining, Veldhuizen, Pathmamanoharan, & Lekkerkerker, 1992). Again, these methods involve delicate chemical modifications of the rod surface. The possibility to apply physical modifications of CNC introducing stabilizing agents and guatanteeing their stable dispersion in organic solvent also after a freeze dried process was reported (Oksman, Mathew, Bondeson, & Kvien, 2006; Heux, Chauve, & Bonini, 2000). The combination of cellulose nanocrystals with other nanostructured materials could lead to many exciting functional properties of hybrid composites based on nanocellulose. The preparation of homogeneous and conductive composite films based on CNC and graphene oxide, with the formation of a conductive film by the application of an electric current has been recently reported (Valentini, Cardinali, Fortunati, Torre, & Kenny, 2013; Gao et al., 2013), analyzing the effect of graphene oxide layers on the arrangement of cellulose nanocrystals. Metal nanoparticles have attracted much research attention with regard to their potential applications in electronic, catalytic, biomedical and sensor materials due to their size-dependent optical, electronic and chemical properties (Campbell, Parker, & Starr, 2002; Sondi & Salopek-Sondi, 2004; Wu, Kuga, & Huang, 2008). It is generally difficult to disperse metallic nanoparticles in a solvent due to their high surface energy and thus high tendency for agglomeration. Therefore, addition of a surfactant or surface modification to the metal nanoparticles is usually required to stabilize in a solvent (Fink, Kiely, Bethell, & Schiffrin, 1998; Harada, Sakurai, Matsushita, Izuoka, & Sugawara, 2002; Yokota, Kitaoka, Opietnik, Rosenau, & Wariishi, 2008; Padalkar et al., 2010). Moreover, it is difficult to fully take advantage of quantum size effects of metal nanoparticles, if they are embedded in polymers. Therefore, the development of immobilization methods of metal nanoparticles on a solid surface is relevant for many advanced applications.

In this paper the nanostructured assembly of silver nanoparticles with cellulose nanocrystals in thin films obtained by spin coating and the investigation of the surface properties of the cellulose/silver organized layers on different substrates are reported Spin coating parameters were modulated and different substrates were considered to determine the best process conditions required to obtain uniform films. Both pristine cellulose nanocrystals (CNC) and surfactant modified crystals (s-CNC) were used for this purpose and different solution concentrations were considered in order to evaluate the effect of modification and concentration on the uniformity of the spin coated cellulose/silver layers. Morphological investigations by field emission scanning electron microscopy and atomic force microscopy were performed and the wettability of the different thin film surfaces was studied. The innovative hybrid thin films reported in this paper constitute an emerging topic in fundamental nanocellulose research.

2. Experimental

2.1. Materials

Commercial silver (Ag) nanopowder, P203, with a size distribution ranging from 20 to 80 nm, was purchased from Cima NanoTech (Corporate Headquarters). Microcrystalline cellulose (MCC, dimensions of 10–15 μm) and chloroform ($CHCl_3$) were supplied by Sigma Aldrich.

2.2. Substrates

Different substrates were considered in order to compare the film properties respect to substrate chemical and conductivity properties. An insulator clean glass, a semi-conductive pristine silicon wafer (SEMIREP, Galliate NO) with resistivity of about 5 Ω cm, cut in squares of about 3 cm × 3 cm, and a conductive fluorinated tin oxide (FTO) were selected as substrates. Moreover conductive substrates of gold deposited (Inficon $X_{TC}/2$ deposition controller) on a 3 cm × 3 cm glass with a gold layer thickness of 15 nm were considered. Treated silicon wafers were also used with a silicon oxide (designed as SiO_x) top layer obtained by oxidising the silicon wafer at ambient atmospheric pressure in an oven at 1000 °C for 30 min (Gunnars, Wågberg, & Cohen Stuart, 2002). Pristine silicon wafers were also treated by means of a radiofrequency plasma treatment, under oxygen flow, using a Sistec, Italy apparatus with Huttinger, Germany power supply at 13.56 MHz. The films (designed as SiO_2) were placed into the stainless steel chamber, then they were evacuated for 1 h until a pressure (P) of 9×10^{-3} Torr. The gas flow was maintained at 60 standard $cm^3\ min^{-1}$. The deposition conditions were P 1.3×10^{-1} Torr, power supply 30 W, bias voltage 275 V and time 20 min.

2.3. Procedures

2.3.1. Cellulose nanocrystal synthesis and modification

Microcrystalline cellulose (MCC) was hydrolyzed in sulphuric acid solution (64% (wt/wt)) at 45 °C for 30 min (Cranston & Gray, 2006). The obtained cellulose nanocrystals (CNC) had the typical dimensions ranging from 100 to 200 nm in length and 15 nm in width (Fortunati et al., 2012a; Petersson, Kvien, & Oksman, 2007). CNC were neutralized by adding drops of 0.25 mol l^{-1} NaOH (Wang, Ding, & Cheng, 2007). Cellulose nanocrystals were modified (s-CNC) as previously reported, by adding acid phosphate ester of ethoxylated nonylphenol surfactant (Beycostat A B09 from CECCA S.A.) to the CNC suspension in portion of 4/1 (wt/wt) (dry content of CNC solution: 0.3%wt) (Fortunati et al., 2012b).

2.3.2. Design of CNC/Ag suspensions

The two final suspensions, containing CNC and s-CNC, were freeze-dried. After freeze drying, chloroform was directly added to the crystals forming 1 wt% suspensions. In order to improve the dispersion of the crystals in chloroform the suspensions were sonicated (Vibracell, 750, Sonics & Materials, Inc USA) for 1 min in an ice bath. Cellulose nanocrystal suspensions, both pristine CNC and modified s-CNC, were diluted to the desired concentration (0.4 wt%) adding pure chloroform.

Silver nanoparticle suspensions were separately prepared by dispersing the Ag powder in $CHCl_3$ at 0.4 wt% and 0.2 wt%, by means of bath sonication treatment (Ultrasonic Bath-mod. Ac-5, EMMEGI, Italy) for 5 h in order to improve the dispersion in the organic solvent. Two different concentrations of Ag were chosen in order to modulate silver percentage respect to cellulose crystals

in the followed binary CNC/Ag system production, and taking into account our previous results on Ag based nanocomposites (Fortunati et al., 2012b).

Binary CNC/Ag or s-CNC/Ag systems were obtained by adding silver nanoparticle suspensions at 0.4 wt% or 0.2 wt% to CNC or s-CNC and the interaction was promoted by a sonication treatment (Vibracell, 750) for 5 min in an ice bath. Four binary suspensions were produced and designed CNC/Ag[1/1] and s-CNC/Ag[1/1] (prepared using cellulose crystal and silver nanoparticle dispersions at 0.4 wt%) and CNC/Ag[1/0.5], s-CNC/Ag[1/0.5] (using 0.4 wt% of cellulose crystal and 0.2 wt% silver nanoparticle dispersion).

2.3.3. Deposition of CNC/Ag spin-coated films

CNC/Ag thin films were prepared by spin coating onto different substrates characterized by different surface properties. Preliminary studies were performed to determine the best conditions to obtain uniform films, varying the volume of the suspension used, the speed (1000 rpm and 2000 rpm) and rotation time of the supports. The final conditions used are: volume 200 μl, speed of 1000 rpm for 1 min.

2.4. Characterization

2.4.1. Chemico-physical characterization of nanomaterials

The microstructure and agglomeration effects of unmodified and surfactant modified cellulose nanocrystals and silver nanoparticles size and morphology after the dispersion in the organic solvent, were investigated by means of field emission scanning electron microscope (FESEM, Supra 25-Zeiss, Germany). Few drops of the different suspensions were cast on to silicon substrate, vacuum dried for 2 h and gold sputtered before the analysis. Photographs of CNC or s-CNC solutions and of binary CNC/Ag and s-CNC/Ag dispersions were taken in order to visually evaluate the effect of surfactant on the stability of different systems.

The absorption spectra of CNC/Ag and s-CNC/Ag cast onto glass coverslip substrate were measured by means of a Perkin-Elmer UV–vis_NIR spectrometer (Lambda-35, USA) which is equipped with an integration sphere for reflectance spectra recording. The spectra were analyzed at room temperature from 200 to 1100 nm in wavelength, with the Kubelka–Munk equation. Infrared spectroscopy was carried out using a Jasco spectrophotometer (FT-IR 615, Japan) in transmission mode, in the range of 4000–400 cm^{-1}.

2.4.2. Film characterization

Field emission scanning electron microscopy (FESEM, Supra 25-Zeiss, Germany) investigations were performed to evaluate the effect of spin coating parameters in order to select the best deposition conditions, to analyze the effects of substrates and the influence of different solution properties or concentrations on the morphology of deposited films. The films were gold sputter coated before and then analyzed at 1 kV.

The morphological features of cellulose deposited films were also investigated using atomic force microscopy (AFM). Cellulose films deposited on silicon and silicon oxide wafer were analyzed in a tapping mode with a scanning probe microscope (Nanoscope IV, Multimode TM from Digital Instruments, USA). Height and phase images were obtained under ambient conditions with a typical scan speed of 0.5–1 line s^{-1}, using a scan head with a maximum range of 100 μm × 100 μm.

Static contact angles (CA) were measured by FTA 1000 Analyser, USA, at room temperature, in order to investigate the wettability of spin coated dispersions as a function of properties and concentrations of binary CNC/Ag and s-CNC/Ag and in relation to the used substrates. The CA was assessed by the sessile drop method in air with drop shape analysis of 20 μl deionized water. Five independent measurements were averaged.

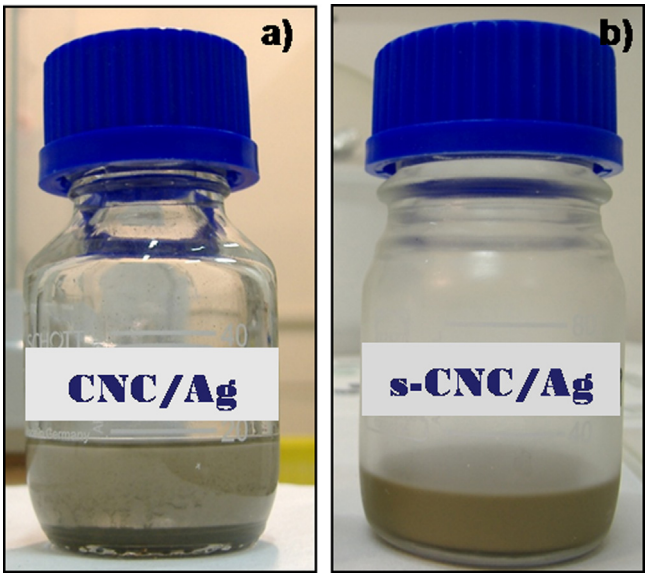

Fig. 1. Visual observation of CNC/Ag (a) and s-CNC/Ag (b) suspension in organic solvent.

3. Results and discussion

3.1. CNC and CNC/Ag suspension characterization

The dispersion and self-ordering properties of cellulose nanocrystals are restricted to aqueous suspensions or dispersions in few organic solvents with high dielectric constant such as dimethyl sulfoxide (DMSO) or ethylene glycol (Turbak et al., 1983). The main reason for such restriction is the electrostatic character of the suspension stability. The difficulty to disperse cellulose structures in organic solvents strongly limits their applications. In the present research, after the hydrolysis process, the two final suspensions, containing unmodified crystals (CNC) and surfactant modified cellulose (s-CNC), were freeze-dried and the cellulose powders were re-dispersed in chloroform.

The ability of the samples to form stable suspensions or gels in chloroform was qualitatively evaluated analyzing the sedimentation of the suspensions in order to establish the effect of modification on the dispersion in the organic solvent. After transferring the suspensions into the testing tubes, photographs were taken at 24 h. These preliminary studies were considered

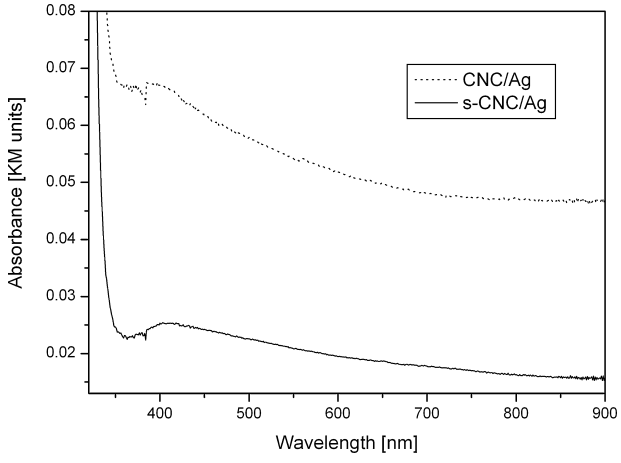

Fig. 2. UV–vis absorption spectra of CNC/Ag and s-CNC/Ag.

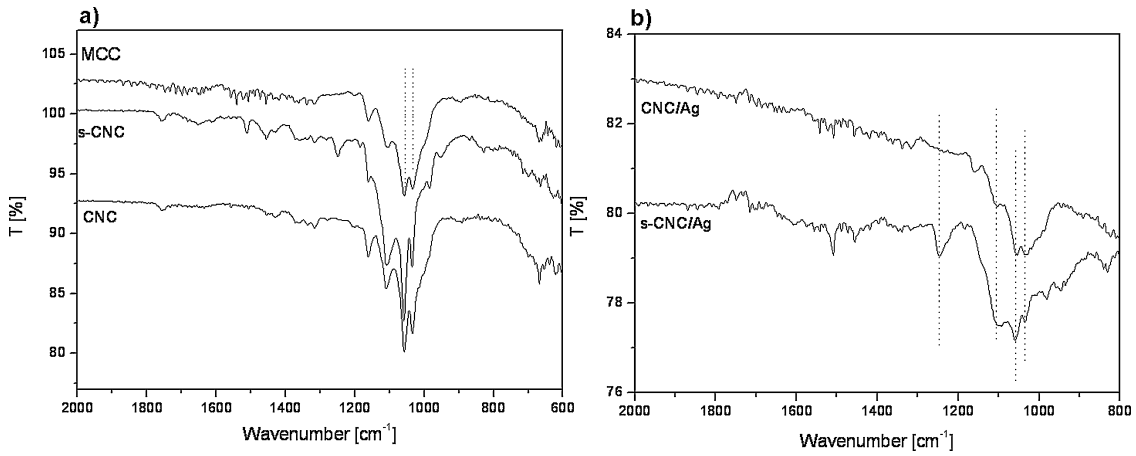

Fig. 3. FT-IR transmission spectra of MCC, CNC and s-CNC (a) and of CNC/Ag and s-CNC/Ag deposited formulations (b).

fundamental for the following CNC/Ag and s-CNC/Ag binary system design and implementation.

The microstructure and agglomeration effects of CNC and s-CNC nanocrystals were previously analyzed (Fortunati et al., 2012b). The formation of aggregates was observed for unmodified cellulose nanocrystals, after modification with the surfactant, a good dispersion in chloroform was observed for the cellulose nanocrystals. The nanocrystals were well individualized without flakes and they show the typical dimensions ranging mostly from 200 to 300 nm in length and around 15 nm in width as previously reported (Fortunati et al., 2012a). The visual observations of CNC and s-CNC liquid suspensions (Fortunati et al., 2012b) confirm this result, with a cloudy-white dispersion in the case of the unmodified CNC solution, while a transparent solution in the modified s-CNC dispersion. The transparency of s-CNC based solution indicates that the dimensions of a major part of cellulose particles in the suspension were below the limit for light-scattering. This was verified by FESEM characterization of the re-dispersed suspensions after freeze-drying (Eyholzer et al., 2010).

Silver nanoparticle solutions were separately prepared by dispersing the Ag at two different concentrations in $CHCl_3$ and then added to the cellulose nanocrystal suspensions in order to obtain CNC/Ag and s-CNC/Ag systems. The visual observations of CNC/Ag and s-CNC/Ag liquid dispersions in the chloroform are reported in Fig. 1. In the case of CNC/Ag with unmodified cellulose (Fig. 1a), aggregates of cellulose and silver particle sedimented at the bottom of the tube were detected after 24 h, while a stable suspension was obtained for modified s-CNC/Ag suspension as shown in Fig. 1b.

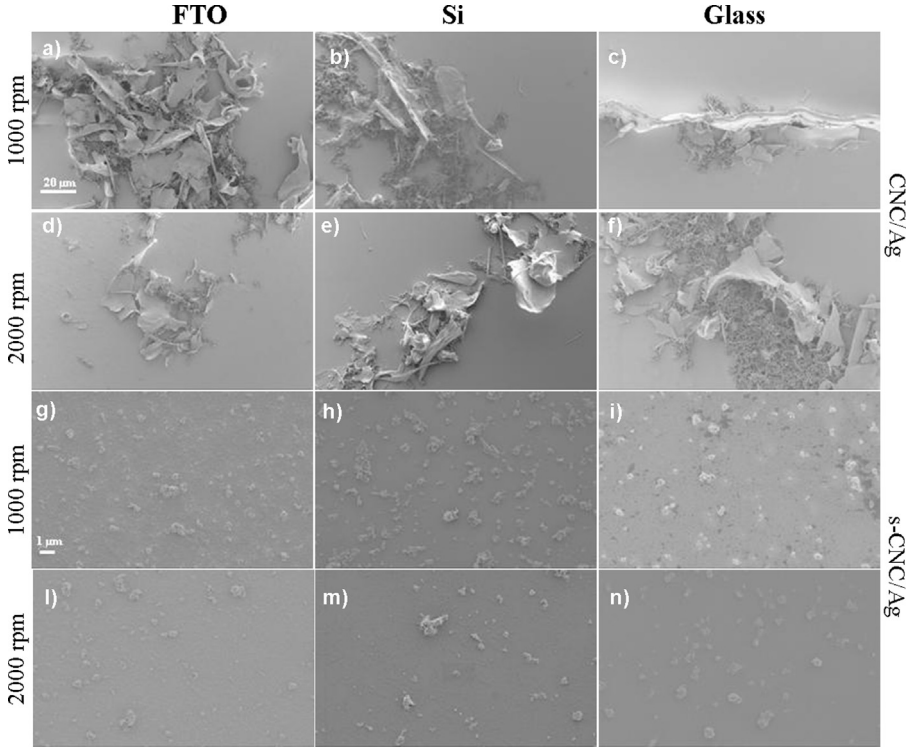

Fig. 4. FESEM images of CNC/Ag (a–f) and s-CNC/Ag (g–n) spun on different substrates: FTO (a, d, g and l); silicon (b, e, h and m) and Glass (c, f, i and n) at 1000 rpm (a–c and g–i) and 2000 rpm (d–f and l–n).

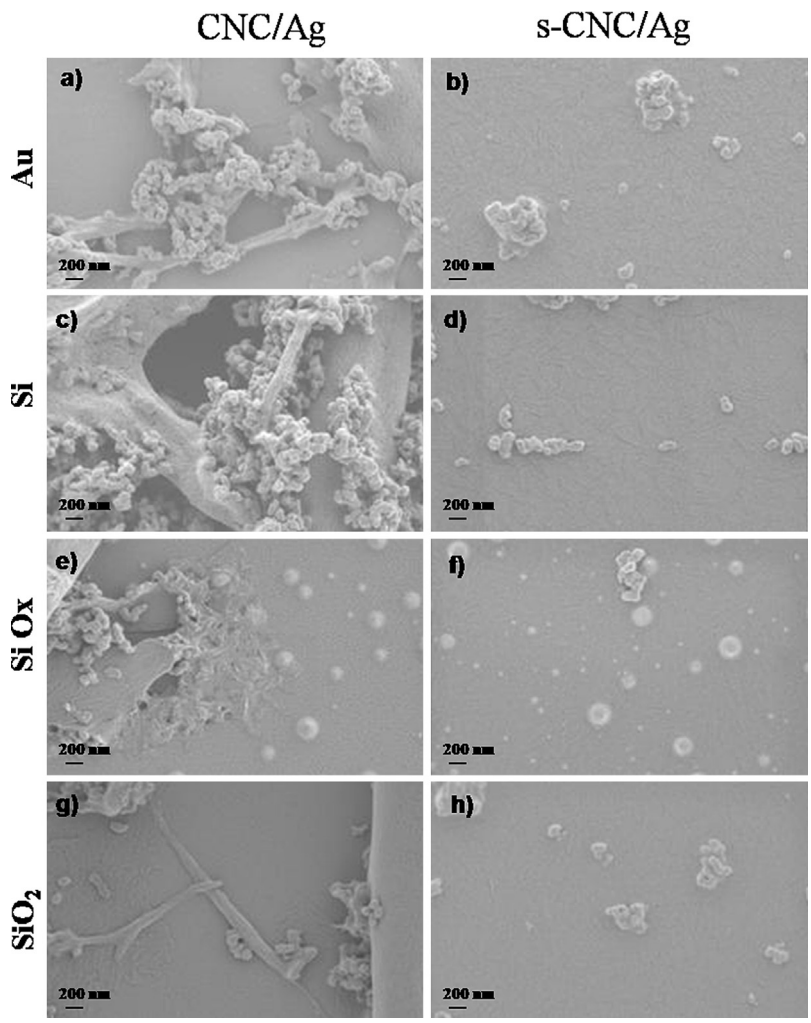

Fig. 5. FESEM images of CNC/Ag (a, c, e and g) and s-CNC/Ag (b, d, f and h) spun at 1000 rpm on Au (a and b), Si (c and d), SiO_x (e and f) and oxygen plasma treated Si (g and h).

This result confirms the enhanced stability obtained for the suspensions with s-CNC/Ag binary systems compared with the unmodified CNC based ones.

Fig. 2 shows the absorption spectra of CNC/Ag and s-CNC/Ag, after deposition on glass coverslip. The spectra present a plasmon band (SPR) peak at 422 nm attributed to colloidal silver nanoparticles (Curry, Nusz, Chilkoti, & Wax, 2005), however the peak is more pronounced in the case of s-CNC/Ag, respect to pristine nanocrystals, where the surfactant presence is able to increase the dispersion of cellulose nanocrystals and facilitate the interaction at nanometer level between silver and cellulose. The surface plasmon resonance band of silver nanoparticles appeared red shifted in the CNC/Ag films, compared to that recorded for the surfactant modified cellulose based films; this behaviour can be probably due to the silver aggregation phenomena induced by the cellulose flakes, that affect the refractive index of the medium around the silver particles, as reported in literature (Kelly, Coronado, Zhao, & Schatz, 2003). This effect is also confirmed by observing the high level of baseline offset at the 800 nm, in the case of CNC/Ag, due to the CNC flake aggregate scattering. Fig. 3 shows the FT-IR transmission spectra of the studied materials; the infrared spectra of microcrystalline cellulose, nanocrystals and surfactant modified nanocrystals (Fig. 3a) show the typical features of cellulose, the broad bands in the 3650–3000 cm^{-1} region are due to O—H stretching vibrations and the peaks at 2900 cm^{-1} correspond to C—H stretching vibrations (Lu & Hsieh, 2010) which are not reported for sake of clarity.

Fig. 3a shows a large absorption between 1136 and 933 cm^{-1}, which results from the contribution of various functional groups, $(C—C)_{str}$, $(C—O)_{str}$ and $(C—O—C)_{st.}$ The region of 800–1500 cm^{-1} is a unique fingerprint region for cellulose where the majority of peaks in that range were found for all samples, indicating that regardless of alkali or acid treatment the cellulose maintained a similar chemical structure to the original untreated species. As shown in Fig. 3a, the vibration of crystals was intensified due to the fact that the change occurred in molecular orientation. The destroyed amorphous region after acid treatment also contributed to the enhancing of the vibration of crystals (1058 cm^{-1} and 1035 cm^{-1}) (Chen et al., 2010; Oh, Yoo, Shin, & Seo, 2005). Fig. 3b compares the spectra of s-CNC and s-CNC/Ag. In the s-CNC the peaks of the surfactant are clearly visible (1245, 1512, 1185, 985 cm^{-1}, but it is important to underline that the surfactant presence does not modify the cellulose nanocrystal order. Also the silver nanoparticles do not change the crystalline order of the cellulose structure.

3.2. Design of spin coating parameters

The effects of different spinning speeds (1000 rpm and 2000 rpm) on the film assembling onto three different substrates, silicon, glass and FTO, are summarized in the FESEM images of the cellulose/silver surfaces (Fig. 4). The assembling of cellulose nanocrystals and silver nanoparticles is strikingly dependent on the surfactant presence and a different behaviour between CNC/Ag

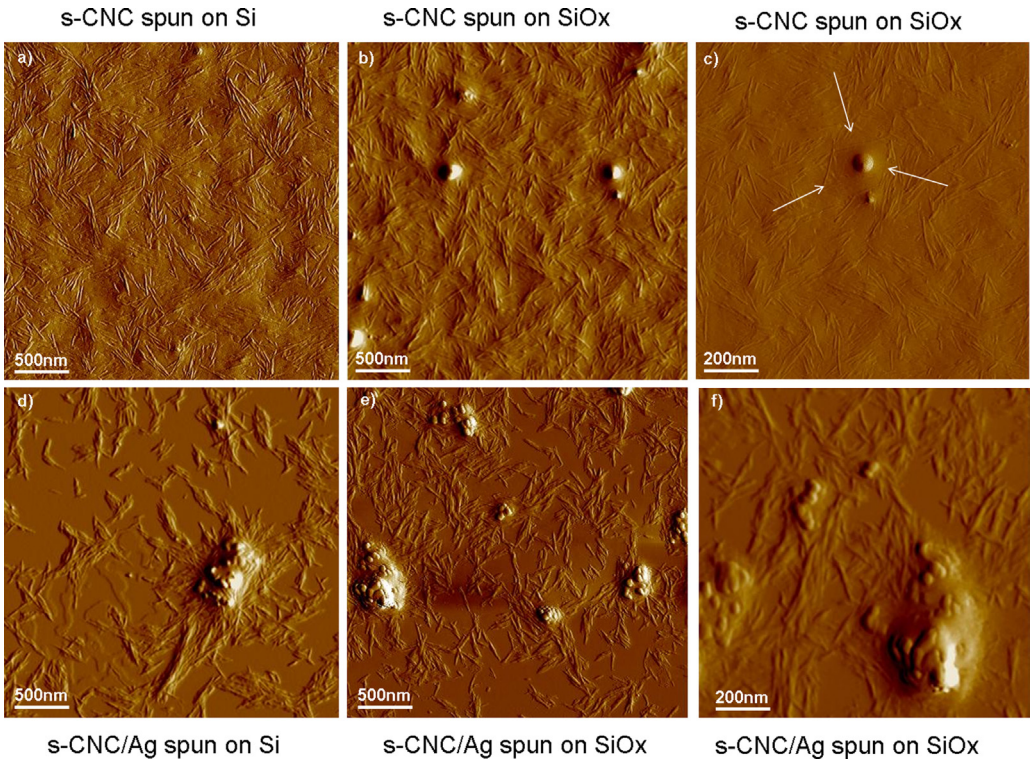

Fig. 6. AFM images of s-CNC and s-CNC/Ag[1/1] layers spin coated (at 1000 rpm) on silicon (a and d) and silicon oxide at different magnification (b and c, e and f).

and s-CNC/Ag solutions was clearly detected after the deposition process. Fig. 4a–f shows the behaviour of unmodified cellulose nanocrystals combined with silver nanoparticles (prepared using cellulose crystal and silver nanoparticle solutions at 0.4 wt%) after spin coating at 1000 rpm (Fig. 4a–c) and 2000 rpm (Fig. 4d–f). The formation of aggregates was observed for unmodified cellulose nanocrystals. The metal nanoparticles tend to form aggregates and to interact with the cellulose flakes but, following the bad dispersion in the organic solvent, the CNC/Ag system does not have the ability to form a uniform film. Instead, the ability of the surfactant modified cellulose to form a stable solution in chloroform permits the formation of a uniform s-CNC/Ag film on the substrate surface (Fig. 4g–n). The individualized acicular nanocrystals assemble in a uniform distribution on different surfaces and the electric properties of the surfaces do not affect the cellulose distribution. Moreover, in the case of s-CNC/Ag, the better dispersion can generate a regular film during the spin coating process that is more homogeneous at 1000 rpm (Fig. 4g–i) respect to 2000 rpm (Fig. 4l–n).

Fig. 4a–i (and l–n), however the conductive or semi-conductive properties of FTO and silicon, respectively, seem to create a better contrast effect during the morphological investigation respect to the insulator glass allowing a more enhanced quality of the images. Moreover, the flat surface of the silicon appears to be ideal for FESEM observation of cellulose nanocrystals. For these reasons, FTO and glass have been abandoned and gold (Au), silicon oxide (SiO_x) and oxygen plasma treated silicon (SiO_2) were introduced in order to modulate or improve the interaction properties between the solution and the substrates.

The evidence reveals that the spinning speed does not influence the capability to form the film but could affect the film thickness and roughness (Kontturi, Thüne, & Niemantsverdriet, 2003; Kontturi et al., 2007). For this reason, a speed of 1000 rpm for one minute was selected as spin coating final parameters in order to analyze the effects of different substrates and concentrations on the formation of the film.

3.3. Film characterization

3.3.1. Effect of different substrates

Fig. 5 shows the FESEM images of CNC/Ag[1/1] and s-CNC/Ag[1/1] spun on four different substrates (gold, silicon, SiO_x and SiO_2) at 1000 rpm for 1 min in order to study the effect of the substrate on the ability to form an homogeneous film and the characteristics of the layer.

The CNC/Ag[1/1] suspension assembles in a discontinuity distribution on all studied substrates (Fig. 5a, c, e and g), with the presence of CNC and silver nanoparticle aggregates. By contrast, modified s-CNC/Ag are able to form a continuous film on different substrates (Fig. 5b, d, f and h) thank to the action of the surfactant rather than by effects of the chemical and electrical properties of the substrate surface. Moreover, the film characteristics obtained with these nanocrystals appear to be more influenced by the topography and the roughness of the substrate than the electrical properties (Fig. 5f).

AFM investigations were carried out for s-CNC and s-CNC/Ag[1/1] spun on silicon and SiO_x in order to deeply study the effect of substrate on the cellulose nanocrystal rearrangement and film morphology. Fig. 6 shows the presence of a continuous s-CNC film on both silicon and silicon oxide surfaces (Fig. 6a and b, respectively). Moreover, at higher magnification of s-CNC deposited on SiO_x (Fig. 6c), cellulose nanocrystals seem to form particular geometries (see arrows in Fig. 6c) around the topography formed by the treatment on silicon surfaces, well underlining the influence of the topography on the cellulose rearrangement on the surface. AFM investigations of s-CNC/Ag[1/1] revealed the presence of a cellulose film with a preferential arrangement of the crystals around the silver agglomerates for both silicon and silicon oxide substrate (Fig. 6d and e, respectively), confirming the results obtained by FESEM analysis. The ability of cellulose nanocrystals to organize into films with a specific order is scientifically intriguing and potentially important for the

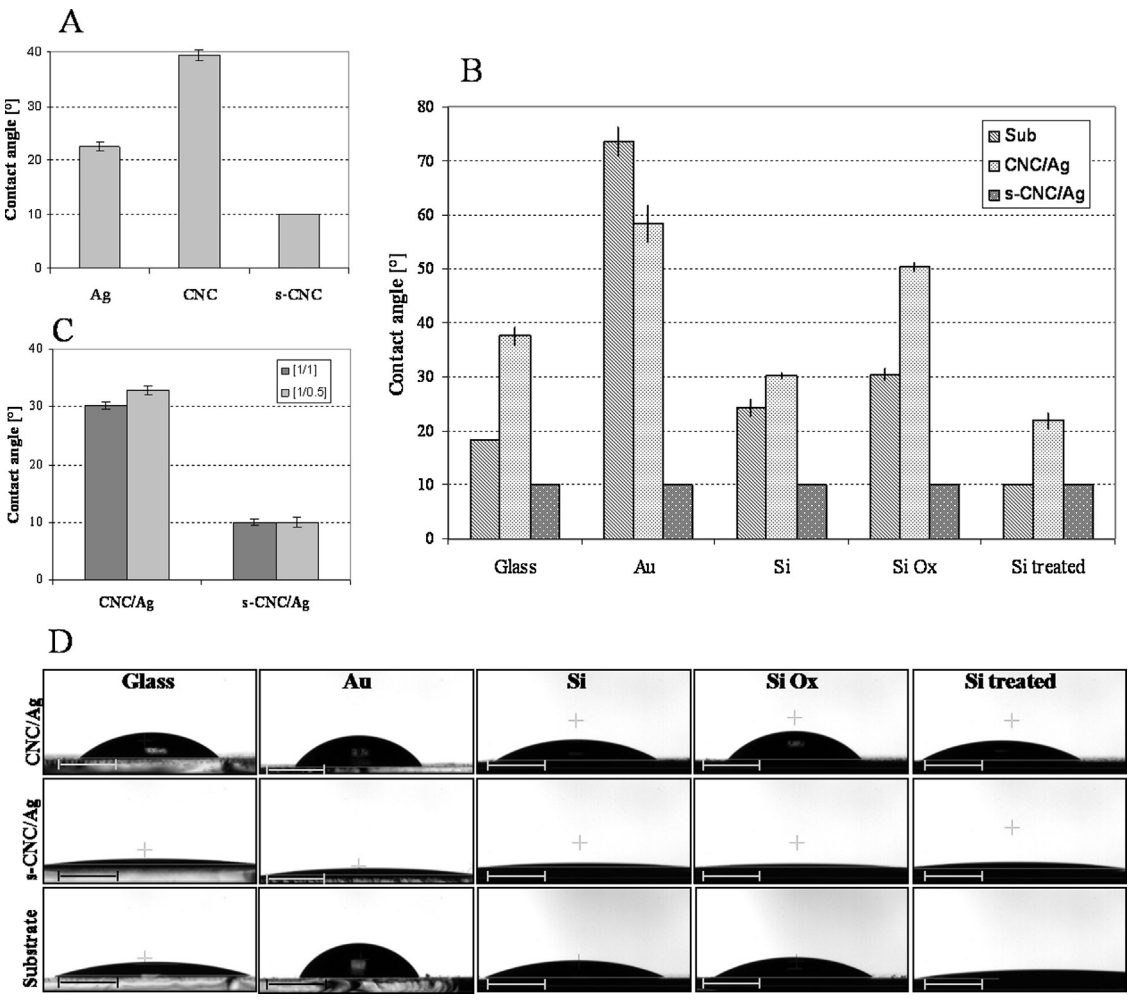

Fig. 7. Contact angle data of single dispersion (Ag, CNC or s-CNC dispersion) spun on silicon (A); contact angle data of CNC/Ag[1/1] and s-CNC/Ag[1/1] dispersion spun on different substrates and pristine substrate (glass, gold, silicon, silicon oxide and silicon plasma treated) (B); comparison of contact angle data of CNC/Ag[1/1], s-CNC/Ag[1/1] and CNC/Ag[1/0.5], s-CNC/Ag[1/0.5], deposited on silicon substrate (C); representative image of water droplet used for contact angle measurements for CNC/Ag[1/1], s-CNC/Ag[1/1] and different substrates (D). All dispersions for contact angle analysis were spun at 1000 rpm.

production of multifunctional materials with attractive optical properties.

The film topography affects also the wettability behaviour of the layers as reported in Fig. 7. All the substrates coated with s-CNC/Ag show a hydrophilic behaviour with contact angles below 10° (Fig. 7B and D) regardless of the value recorded for the single substrate, while a different behaviour was detected for CNC/Ag system. The contact angle of CNC/Ag[1/1] film spun on glass, silicon, SiO_x and SiO_2, 38°, 30°, 50° and 22°, respectively, are higher than the value measured for the pristine substrates (respectively 18°, 24°, 30° and <10°). However, in the case of gold, which has a contact angle of 74°, the film is a little more hydrophilic (58°). Furthermore, analysing the data of contact angle of individual solutions (Fig. 7A) and binary solutions on silicon (Fig. 7B), it is evident that a good interaction between the CNC and Ag nanoparticles occurs. The contact angle for silver and CNC on silicon is 22° and 39°, respectively, while it was 30° in the case of CNC/Ag[1/1] binary system. The different arrangements of the cellulose nanocrystals on the different substrates may be due to differences in the wettability of the substrates. This effect is evident in the CNC/Ag film deposition, while the surfactant effect predominates in the s-CNC/Ag system.

3.3.2. *Effect of the suspension concentration*

Two different concentrations of the cellulose/silver binary systems were considered in this part of the research in order to improve the homogeneity of film. The morphological and wettability properties of CNC/Ag[1/0.5] and s-CNC/Ag[1/0.5] systems, obtained using a lower concentration of silver nanoparticles (0.2 wt%), were investigated with respect to the CNC/Ag[1/1] and s-CNC/Ag[1/1] (produced with 0.4 wt% of silver particles respect to the organic solvent) and the influence of the silver concentration on the film properties were studied. Fig. 8 shows the FESEM images of cellulose/silver films spun on silicon wafer at 1000 rpm. Fig. 8a and d show the interaction between unmodified CNC and silver nanoparticles that is better in the case of CNC/Ag[1/0.5], at lower concentration of silver due to the reduced agglomeration of Ag particles. This is confirmed by the fact that also in the case of s-CNC/Ag the silver nanoparticle aggregates are smaller for [1/0.5] than [1/1] concentration (Fig. 8b–c and e–f). The high magnification images (Fig. 8c and f) show how the reduced concentration of silver allows the formation of uniform and homogenous s-CNC film with little aggregates of silver nanoparticles.

Contact angle measurements show hydrophilicity for s-CNC/Ag[1/0.5] films also in the case of lower concentration of silver (Fig. 7C and A) confirming the result obtained for the s-CNC/Ag[1/1] system and highlighting that the wettability properties are strongly influenced by the cellulose nanocrystal nature and in a less evidence by the silver concentration. On the other side the contact angle of CNC/Ag[1/0.5] comes close to the value obtained for CNC/Ag[1/1] system (Fig. 7C).

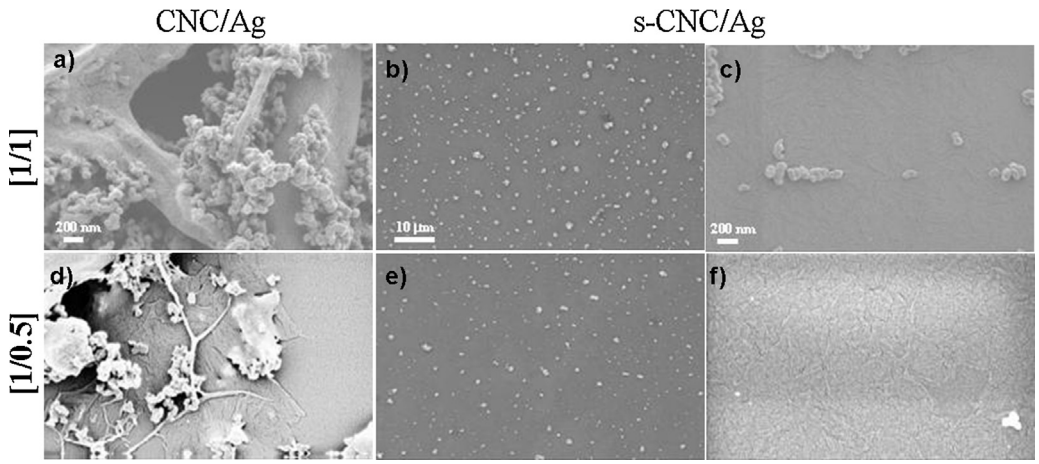

Fig. 8. FESEM images of CNC/Ag (a and d) and s-CNC/Ag (b and c, e and f) at different concentration, spun on silicon at 1000 rpm.

4. Conclusions

This work revealed that the presence of a surfactant allows to obtain stable suspensions of cellulose nanocrystals as well as of binary systems formed by cellulose nanocrystals and silver nanoparticles in chloroform. We have demonstrated the dominant effect of surfactant nanocrystal modifications on the arrangement of spin coated layers of cellulose and cellulose/silver systems.

The UV–vis and FT-IR analyses have shown that the molecular structure of cellulose remains the same after the nanocrystal synthesis and modification, but the AFM and FESEM measurements suggest strong changes in morphology, thus supramolecular rearrangement. This rearrangement seems to be a more complex phenomenon affected by the presence of silver nanoparticles. The formation of a film by spin coating technique depends on the surfactant presence and it was not influenced by process parameters and substrate conductivity, whereas the s-CNC film behaviour was affected by substrate roughness and topography and by the presence and concentration of silver nanoparticles. More specifically, the lower concentration of Ag nanoparticles facilitates the uniformity of cellulose films. Moreover, wettability studies confirm the homogeneity of s-CNC based films on all the considered substrates, the good interaction between cellulose crystals and silver nanoparticles and underline that the hydrophilicity depends on the cellulose nature. The homogeneous distribution of cellulose nanocrystals on silicon based substrates renders spin coating a superior method applied in constructing cellulose nanocrystal layers. This work points out that simple spin coating together with a correctly chosen substrate removes the problem of aggregation. The combination of cellulose nanocrystals with silver NPs at the moment can be the basis of “smart paper”, opening the way toward new perspectives in different domains with a large number of applications, as in biomedical applications, due to the antibacterial character of silver nanoparticles, enabling their use in wound dressing materials, body wall repairs, tissue scaffolds, or even antimicrobial filters.

Acknowledgements

Authors wish to thank the Institute of Polymer Science and Technology, CSIC, Spain, and Dr. Laura Peponi for AFM measurements.

References

Budkowski, A. (1999). Interfaces crystallization viscoelasticity. *Advances in Polymer Science*, *148*, 1–111.

Buining, P. A., Veldhuizen, Y. S., Pathmamanoharan, C., & Lekkerkerker, H. N. W. (1992). Preparation of a non-aqueous dispersion of sterically stabilized boehmite rods. *Colloids and Surfaces*, *64*, 47–55.

Campbell, D. T., Parker, S. C., & Starr, D. E. (2002). The effect of size-dependent nanoparticle energetics on catalyst sintering. *Science*, *298*, 811–814.

Cavailleí, J. Y., Chanzy, H., Fleury, E., & Sassi, J. F. (1997). PCT int. appl. In *WO 97 12,917*.

Chen, J., Nan, K., Yin, S., Wang, Y., Wu, T., & Zhang, Q. (2010). Characterization and biocompatibility of nanohybrid scaffold prepared via in situ crystallization of hydroxyapatite in chitosan matrix. *Colloids and Surface B: Biointerfaces*, *81*, 640–647.

Cranston, E. D., & Gray, D. G. (2006). Morphological and optical characterization of polyelectrolyte multilayers incorporating nanocrystalline cellulose. *Biomacromolecules*, *7*, 2522–2530.

Curry, A., Nusz, G., Chilkoti, A., & Wax, A. (2005). Substrate effect on refractive index dependence of plasmon resonance for individual silver nanoparticles observed using darkfield microspectroscopy. *Optic Express*, *13*, 2668–2677.

Dong, X. M., Revol, J. F., & Gray, D. G. (1998). Effect of microcrystallite preparation conditions on the formation of colloid crystals of cellulose. *Cellulose*, *5*, 19–32.

Edgar, C. D., & Gray, D. G. (2002). Influence of dextran on the phase behavior of suspensions of cellulose nanocrystals. *Macromolecules*, *35*, 7400–7406.

Eyholzer, Ch, Bordeanu, N., Lopez-Suevos, F., Rentsch, D., Zimmermann, T., & Oksman, K. (2010). Preparation and characterization of water-redispersible nanofibrillated cellulose in powder form. *Cellulose*, *17*, 19–30.

Fink, J., Kiely, C. J., Bethell, D., & Schiffrin, D. J. (1998). Self-organization of nanosized gold particles. *Chemistry of Materials*, *10*, 922–926.

Fortunati, E., Armentano, I., Zhou, Q., Iannoni, A., Saino, E., Visai, L., Berglund, L. A., & Kenny, J. M. (2012). Multifunctional bionanocomposite films of poly(lactic acid) cellulose nanocrystals and silver nanoparticles. *Carboydrate Polymers*, *87*, 1596–1605.

Fortunati, E., Armentano, I., Zhou, Q., Puglia, D., Terenzi, A., Berglund, L. A., & Kenny, J. M. (2012). Microstructure and nonisothermal cold crystallization of PLA composites based on silver nanoparticles and nanocrystalline cellulose. *Polymer Degradation & Stability*, *97*, 2027–2036.

Gao, K., Shao, Z., Wu, X., Wang, X., Li, J., Zhang, Y., Wang, W., & Wang, F. (2013). Cellulose nanofibers/reduced graphene oxide flexible transparent conductive paper. *Carbohydrate Polymers*, *97*, 243–251.

Gunnars, S., Wågberg, L., & Cohen Stuart, M. A. (2002). Model films of cellulose: I, Method development and initial results. *Cellulose*, *9*, 239–249.

Gunter, P. L. J., Niemantsverdriet, J. W., Ribeiro, F. H., & Somorjai, A. (1997). Surface science approach to modeling supported catalysts. *Catalysis Reviews Science and Engineering*, *39*, 77–168.

Harada, G., Sakurai, H., Matsushita, M. M., Izuoka, A., & Sugawara, T. (2002). Preparation and characterization of gold nano-particles chemisorbed by *p*-radical thiols. *Chemistry Letters*, *31*, 1030–1031.

Heux, L., Chauve, G., & Bonini, C. (2000). Nonflocculating and chiral-nematic self-ordering of cellulose microcrystals suspensions in nonpolar solvents. *Langmuir*, *16*, 8210–8212.

Jiang, P., & McFarland, M. J. (2004). Large-scale fabrication of wafer-size colloidal crystals, macroporous polymers and nanocomposites by spin-coating. *Journal of American Chemical Society*, *126*, 13778–13786.

Kaplan, D. L. (1998). In D. L. Kaplan (Ed.), *In biopolymers from renewable resources* (pp. 1–29). Berlin: Springer.

Kelly, K. L., Coronado, E., Zhao, L. L., & Schatz, G. C. (2003). The optical properties of metal nanoparticles: The influence of size, shape, and dielectric environment. *Journal of Physical Chemistry B*, *107*, 668–677.

Klemn, D., Heublein, B., Fink, H. P., & Bohn, A. (2005). Cellulose: Fascinating biopolymer and sustainable raw material. *Angewandte Chemie International Edition*, *44*, 3358–3393.

Kontturi, E., Johansson, L. S., Kontturi, K. S., Ahonen, P., Thüne, P. C., & Laine, J. (2007). Cellulose nanocrystal submonolayers by spin coating. *Langmuir*, *23*, 9674–9680.

Kontturi, E., Thüne, P. C., Alexeev, A., & Niemantsverdriet, J. W. (2005). Introducing open films of nanosized cellulose—Atomic force microscopy and quantification of morphology. *Polymer*, *46*, 3307–3317.

Kontturi, E., Thüne, P. C., & Niemantsverdriet, J. W. (2003). Novel method for preparing cellulose model surfaces by spin coating. *Polymer*, *44*, 3621–3625.

Lee, S. S., Lee, K. B., & Hong, J. D. (2003). Evidence for spin coating electrostatic self-assembly of polyelectrolytes. *Langmuir*, *19*, 7592–7596.

Lu, P., & Hsieh, Y. L. (2010). Preparation and properties of cellulose nanocrystals: Rods, spheres, and network. *Carbohydrate Polymer*, *82*, 329–336.

Mark, H. (1980). Fifty years of cellulose research. *Cellulose Chemistry and Technology*, *14*, 569–581.

Norman, K., Ghanbari-Siahkali, A., & Larsen, N. B. (2005). Studies of spin-coated polymers films. *Annual Reports on the Progress of Chemistry, Section C: Physical Chemistry*, *101*, 174–201.

Oh, S. Y., Yoo, D. I., Shin, Y., & Seo, G. (2005). FTIR analysis of cellulose treated with sodium hydroxide and carbon dioxide. *Carbohydrate Research*, *340*, 417–428.

Oksman, K., Mathew, A. P., Bondeson, D., & Kvien, I. (2006). Manufacturing process of cellulose whiskers/polylactic acid nanocomposite. *Composite Science and Technology*, *66*, 2776–2784.

Padalkar, S., Capadona, J. R., Rowan, S. J., Weder, C., Won, Y. H., Stanciu, L. A., & Moon, R. J. (2010). Natural biopolymers: Novel templates for the synthesis of nanostructures. *Langmuir*, *26*, 8497–8502.

Petersson, L., Kvien, I., & Oksman, K. (2007). Structure and thermal properties of poly(lactic acid)/cellulose whiskers nanocomposite materials. *Composite Science and Technology*, *67*, 2535–2544.

Qin, S., Matyjaszewski, K., Xu, H., & Sheiko, S. S. (2003). Synthesis and visualization of densely grafted molecular brushes with crystallizable poly(octadecyl methacrylate) block segments. *Macromolecules*, *36*, 605–612.

Revol, J. F., Bradford, H., Giasson, J., Marchessault, R. H., & Gray, D. G. (1992). Helicoidal self-ordering of cellulose microfibrils in aqueous suspension. *International Journal of Biological Macromolecules*, *14*, 170–172.

Singh, A., & Mukherjee, M. (2004). Discrete film thickness in polyacrylamide-CdS nanocomposite ultrathin films. *Physical Review E: Statistical, Nonlinear, and Soft Matter Physics*, *70*, 051608.

Sondi, I., & Salopek-Sondi, B. J. (2004). Silver nanoparticles as antimicrobial agent: A case study on E. coli as a model for Gram-negative bacteria. *Colloid Interface Science*, *275*, 177–182.

Sun, B., & Sirringhaus, H. (2006). Surface tension and fluid flow driven self-assembly of ordered ZnO nanorod films for high-performance field effect transistors. *Journal of American Chemical Society*, *128*, 16231–16237.

Turbak, A. F., Snyder, F. W., & Sandberg, K. R. (1983). Microfibrillated cellulose, a new cellulose product: Properties, uses, and commercial potential. Applied polymer symposium. *Journal of Applied Polymer Science*, *37*, 815–827.

Valentini, L., Cardinali, M., Fortunati, E., Torre, L., & Kenny, J. M. (2013). A novel method to prepare conductive nanocrystalline cellulose/graphene oxide composite films. *Materials Letters*, *105*, 4–7.

Wang, N., Ding, E., & Cheng, R. (2007). Thermal degradation behaviors of spherical cellulose nanocrystals with sulfate groups. *Polymer*, *48*, 3486–3493.

Wu, M., Kuga, S., & Huang, Y. (2008). Quasi-one-dimensional arrangement of silver nanoparticles templated by cellulose microfibrils. *Langmuir*, *24*, 10494–10497.

Xia, D., & Brueck, S. R. J. (2004). A facile approach to directed assembly of patterns of nanoparticles using interference lithography and spin coating. *Nano Letters*, *4*, 1295–1299.

Yokota, S., Kitaoka, K., Opietnik, M., Rosenau, T., & Wariishi, H. (2008). Synthesis of gold nanoparticles for in situ conjugation with structural carbohydrates. *Angewandte Chemie International Edition*, *47*, 9866–9869.

Yoon, J., Ree, M., Hwang, Y., Lee, S. W., Lee, B., Kim, J. S., Kim, H., & Magonov, S. N. (2004). Formation of a two-dimensionally well-ordered monolayer of a peptide oligomer by a simple spin-coating process. *Langmuir*, *20*, 544–549.